Biophysical Journal, Volume 99

Supporting Material

DnaB helicase activity is modulated by DNA geometry and force

Noah Ribeck, Daniel L. Kaplan, Irina Bruck, and Omar A. Saleh

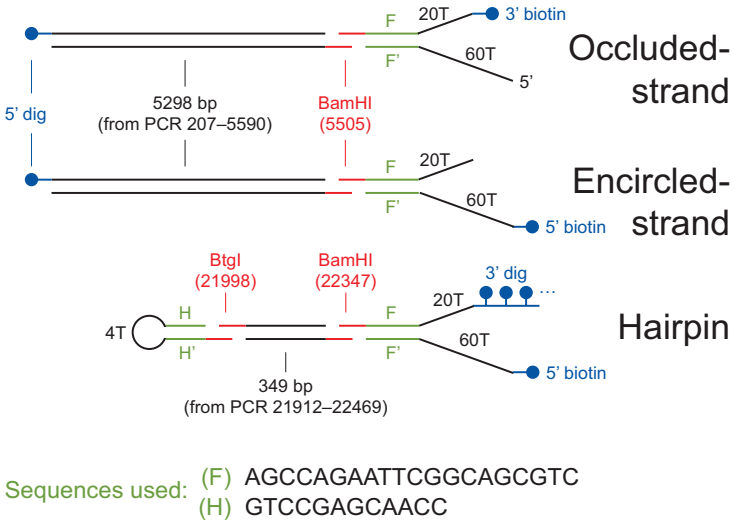

Figure S1. Illustration of the assembly of tetherable DNA substrates as described in the Methods. Numbers in parentheses refer to the location in the λ phage genome from which the specified sequences were derived. Gaps indicate points of ligation. The total length of the double-stranded DNA in each assembly is 5322 bp for the occluded- and encircled-strand geometries, and 389 bp for the hairpin.

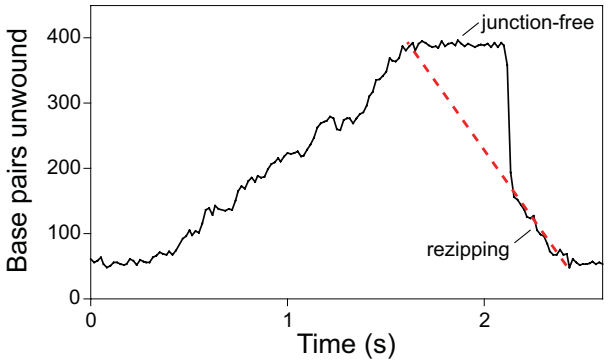

Figure S2. Example hairpin trace illustrating that the rezipping rate is equal to translocation rate on ssDNA. At high applied force, the lifetime of the open state of the hairpin is sometimes comparable to the time it takes for DnaB to translocate along the second half of the hairpin. This results in a measured pause in bead motion (labeled here as "junction-free"), with the hairpin transiently remaining in the open state while the helicase freely translocates along ssDNA without the junction nearby. The hairpin then abruptly closes up to the position of DnaB, at which point typical gradual rezipping resumes. The distance of the abrupt hairpin closing divided by the hairpin open time provides an estimate of the junction-free translocation rate of the helicase. 10 such events were observed (see Table S1).

Event #	Force (pN)	Junc-free rate (bp/s)	Rezipping rate (bp/s)	Rezipping/ Junc-free
1	11.3	458	399	0.87
2	13.1	544	455	0.84
3	13.8	498	535	1.07
4	13.8	586	573	0.98
5	14.2	117	226	1.93
6	14.2	226	250	1.10
7	15.1	496	497	1.00
8	15.1	212	347	1.64
9	15.1	242	364	1.51
10	15.1	318	279	0.88

Table S1. Junction-free translocation rates compared to rezipping. Of 10 observed events of the type shown in Fig. S2, 7 have junction-free velocities equal, to within experimental error, to the rezipping rate that immediately follows within the same event (shaded). For the remaining 3 events, the rezipping rate was significantly greater than the junction-free rate. Since these events were in the minority, we conclude they are likely caused by pauses during junction-free translocation which are undetectable during the transiently open state and would lead to an underestimate of the translocation rate. Therefore, as was similarly shown for T4 gp41 helicase (1), we conclude that the closing junction the presence of the junction directly behind DnaB does not prevent any backstepping or affect the translocation of the helicase along ssDNA in any significant way.

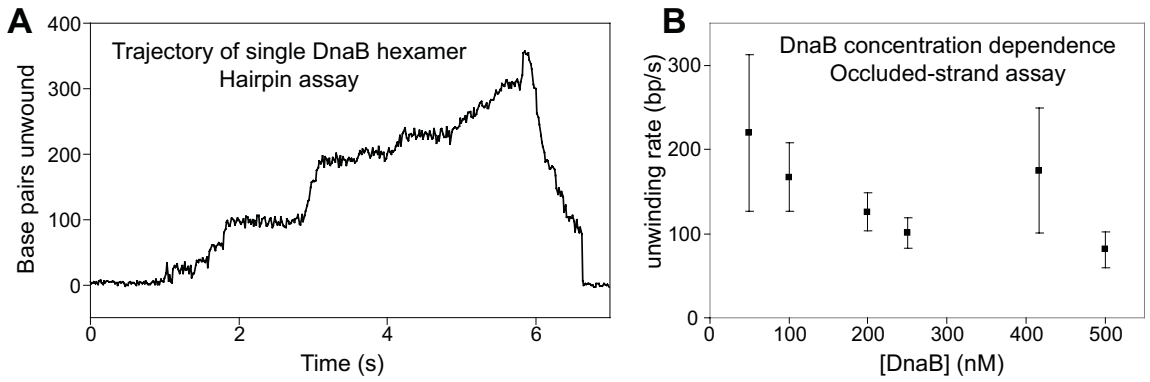

Figure S3. Data supporting the single-molecule condition. (*A*) Example trace of single-hexamer activity. Using a hairpin with enough loading area (20 nt) for only a single DnaB hexamer (2), protein was added in a solution containing helicase buffer and 200 μM AMP-PNP instead of ATP, allowing only a single DnaB hexamer to load. After a 20 minute incubation, excess protein was washed out with 200 uL (~8 sample volumes) of the same solution, and 5 mM ATP was added to out-compete the AMP-PNP. The activity of this single hexamer at 11.3 pN (unwinding rate, translocation rate, pausing, and processivity) is quantitatively similar to others described in this study, indicating that a single DnaB hexamer is capable of the events described here. (*B*) Unwinding rate in the occluded-strand assay as a function of DnaB concentration. If our data included activity by multiply bound helicases, we would expect to see a strong concentration dependence: at higher concentration, events should display faster unwinding, assuming that multiple helicases travel faster than one. However, there is no significant concentration dependence on the unwinding rate.

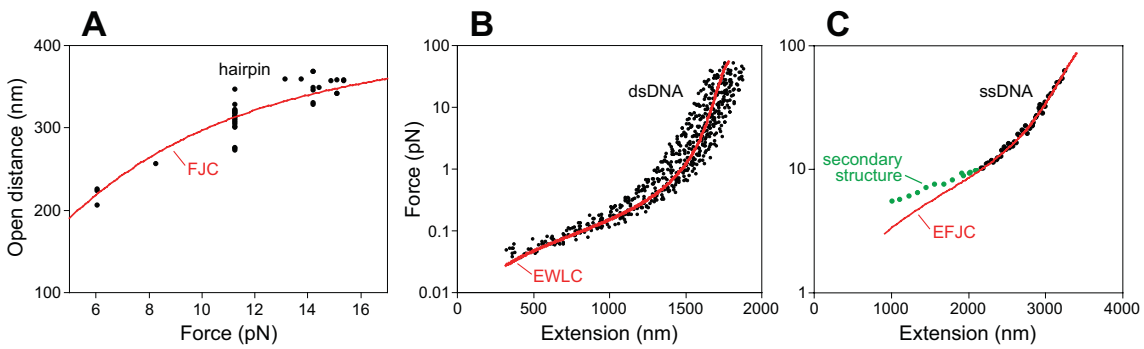

Figure S4. Force-extension relations used for calibration of helicase position to bead position and for calculation of $\Delta G_{\mathrm{bp}}(F)$.

(*A*) Force-extension curve of ssDNA in the hairpin assay. The measured extension is the total displacement Nx_{ss} of the bead upon unwinding all $N = 389$ bp over a range of forces (1). The data are fit to the freely jointed chain (FJC) model of polymer elasticity (3):

$$\frac{x_{\mathrm{ss}}}{L_{\mathrm{ss}}} = \coth\left(\frac{Fb_{\mathrm{ss}}}{k_B T}\right) - \frac{k_B T}{Fb_{\mathrm{ss}}}, \qquad [1]$$

giving a Kuhn length $b_{\mathrm{ss}} = 1.16 \pm 0.03$ nm, where $L_{\mathrm{ss}} = 0.58$ nm is the contour length of a single base. Forces are sufficiently high in this assay ($F > k_B T / b_{\mathrm{ss}} = 3.4$ pN) for self-interaction of the polymer chain to be negligible (4, 5), and thus the FJC is an accurate representation.

(*B*) Force-extension curve of the dsDNA in the fork assay. We used power spectrum methods (6) to measure force vs. extension in the helicase buffer. The data are fit to the extensible worm-like chain model (7-9):

$$F = \left(\frac{k_B T}{l_{\mathrm{p}}}\right)\left(\frac{1}{4(1 - x_{\mathrm{ds}}/L_{\mathrm{ds}} + F/K_{\mathrm{ds}})^2} - \frac{1}{4} + \frac{x_{\mathrm{ds}}}{\mathrm{L}_{\mathrm{ds}}} - \frac{F}{K_{\mathrm{ds}}}\right), \qquad [2]$$

giving a persistence length $l_{\mathrm{p}} = 46.1 \pm 0.1$ nm, where $L_{\mathrm{ds}} = 0.34$ nm is the contour length of a single base pair, and $K_{\mathrm{ds}} = 1300$ pN (10, 11) is the elastic modulus of dsDNA.

(*C*) Force-extension curve of the ssDNA in the fork assay. We obtained ssDNA by PCR of the 5.3 kb segment from the fork assay with two 5' biotin labeled primers and labeling the 3' ends with terminal transferase and digoxigenin labeled nucleotides. We then heated the DNA to 95°C for 2 minutes to melt the strands, diluted to 200 pM and added to the flow cell with antidigoxigenin non-specifically bound to the glass surface. We used power spectrum methods (6) to measure force vs.extension in the helicase buffer. The data are fit to the extensible freely jointed chain (12) in the range $F > 10$ pN, where no secondary structure forms (13):

$$\frac{x_{ss}}{L_{ss}} = \left(\coth\left(\frac{Fb_{ss}}{k_B T} \right) - \frac{k_B T}{Fb_{ss}} \right)\left(1 + \frac{F}{K_{ss}} \right), \qquad [3]$$

giving a Kuhn length $b_{ss} = 1.23 \pm 0.01$ nm, where $L_{ss} = 0.58$ nm is the contour length of a single base pair, and $K_{ss} = 800$ pN (12) is the elastic modulus of ssDNA.

DNA geometry	Processivity (bp)
Occluded-strand	1199 ± 102
Encircled-strand	870 ± 160

Table S2. Processivities measured in the fork assays. The 5.3 kb DNA substrate was observed to be unwound completely only once in the 92 total events recorded. These processivities are significantly less than the 10.5 kb processivity shown for leading strand synthesis of the *E. coli* replisome in a single-molecule experiment (14), indicating that the presence of DNA polymerase III holoenzyme greatly stimulates helicase activity. In that study, no unwinding activity was observed with DnaB alone, although the ~1 kb resolution of the experiment was not sufficient to observe the length of many of the events that we report here. Although the processivity we measure is decreased significantly from that of the entire replisome, it is inconsistent with the result of a single-turnover bulk study that measured the processivity of DnaB alone to be ~9 bp (15). The value we report here is consistent with bulk studies of the *E. coli* replisome that have shown that DnaB continues to unwind ~1 kb of dsDNA after becoming uncoupled from the holoenzyme by a lesion on the leading strand (16-18).

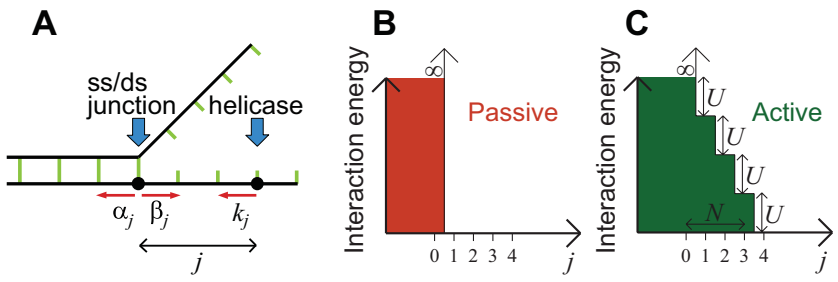

Figure S5. Theoretical model of helicase unwinding.

(*A*) Illustration of the theoretical model of helicase unwinding (19, 20). The helicase steps forward at rate k_j, while the dsDNA fluctuates open at rate α_j and closed at rate β_j. These rates depend on the separation j between the helicase and the ss/dsDNA junction.

(*B*) In the passive model, there is no interaction between the helicase and the ss/dsDNA junction, and thus proximal base pairs remain as stably bound as they are with no helicase present. The energy landscape is thus characterized by a hard wall at $j = 0$. The "passive" unwinding rate is $u_{\text{passive}} = nk \exp(-n\Delta G_{\text{bp}} / k_B T)$ (see main text), where n is the step size, and k is the helicase stepping rate on ssDNA ($k = r/n$). We have assumed here, as we do throughout, that dsDNA breathing dynamics are much faster than helicase stepping, and that there is no backstepping.

(*C*) In the active model, we add an additional repulsive interaction energy between the helicase and the junction over a range of N bp, decreasing linearly with separation distance by an amount U per bp. The potential does not affect the system until the helicase is within N bp of the junction, at which point the repulsion both slows the forward rate of the helicase and destabilizes the proximal base pair. The translocation rate r is slowed by a factor $\exp(-naU/k_B T)$, where a is a dimensionless parameter ($0 < a < 1$) that indicates whether the primary effect of the interaction is to either facilitate unwinding ($a \to 0$) or prevent rebinding of base pairs ($a \to 1$). The binding free energy of the proximal base pair is decreased by an amount U, thus making it more likely to be open than due to thermal fluctuation alone. As previously (20), we derive a

predicted unwinding rate, generalized to a helicase with step size n (note that the coordinate j is shifted by N compared to the Betterton and Julicher formalism), based on the parameters of this repulsive interaction (from here on, U/k_BT will simply be written as U for convenience). The "active" unwinding rate is calculated by:

$$u_{\text{active}} = n\sum_j k_j P_j \,, \qquad [4]$$

where P_j is the probability that the helicase and ss/dsDNA junction are separated by j nt, and k_j is the helicase stepping rate at separation j. The probability is given by:

$$P_j = \begin{cases} 0, & j < 1, \\ Ac^j e^{(j-N-1)U}, & 1 \le j \le N, \\ Ac^j, & j > N, \end{cases} \qquad [5]$$

where $c = \exp(-\Delta G_{\text{bp}}/k_BT)$, and the normalization constant A is determined by $\sum_j P_j = 1$. The helicase stepping rate is given by:

$$k_j = \begin{cases} 0, & j \le n, \\ ke^{-anU}, & n < j \le N \\ ke^{-a(n+N+1-j)U}, & N < j \le N+n, \\ k, & j > N+n, \end{cases} \qquad [6]$$

where a is the interaction parameter (see above). Then we have:

$$u_{\text{active}} = nkA\left[e^{-anU}\left(\sum_{j=n+1}^{N} c^j e^{(j-N-1)U} + \sum_{j=N+1}^{N+n} c^j e^{a(j-N-1)U} \right) + \sum_{j=N+n+1}^{\infty} c^j \right], \qquad [7]$$

which can be written as:

$$\begin{aligned} u_{\text{active}} &= nkc^n\alpha \\ &= rc^n\alpha \\ &= u_{\text{passive}}\alpha, \end{aligned} \qquad [8]$$

where the factor α is given by:

$$\alpha(U,N,a,n,c) = \frac{1+(1-c)e^{-anU}\left(\sum_{j=1}^{n} c^{-j}e^{-a(j-n)U} + \sum_{j=n+1}^{N} c^{-j}e^{-(j-n)U}\right)}{1+(1-c)\sum_{j=1}^{N} c^{-j}e^{-jU}}. \qquad [9]$$

Therefore, the "active" interaction energy increases helicase unwinding by a factor $\alpha > 1$.

	n \ N	1	2	3	4	5	6	7	8	9	10
Occluded-strand U/k_BT	1	1.9	1.6	1.5	1.4	1.4	1.4	1.4	1.4	1.4	1.4
	2	5.2	2.8	2.3	2.2	2.1	2.0	2.0	2.0	2.0	2.0
	3	5.0	4.5	3.2	2.7	2.5	2.4	2.4	2.3	2.3	2.3
	4	4.7	4.3	4.2	3.6	2.9	2.7	2.6	2.6	2.5	2.5
Occluded-strand χ^2	1	0.56	0.47	0.50	0.54	0.57	0.60	0.61	0.63	0.63	0.64
	2	17.89	0.65	0.82	1.19	1.58	1.93	2.23	2.49	2.70	2.88
	3	26.72	19.90	0.90	0.94	1.30	1.69	2.05	2.35	2.61	2.82
	4	28.12	27.06	21.44	1.53	1.10	1.25	1.51	1.77	2.01	2.22
Hairpin U/k_BT	1	0.5	0.4	0.3	0.3	0.3	0.3	0.3	0.3	0.3	0.3
	2	4.7	1.4	1.1	1.0	0.9	0.8	0.8	0.8	0.8	0.7
	3	4.2	3.9	1.9	1.4	1.3	1.2	1.1	1.1	1.1	1.1
	4	4.0	3.5	3.5	2.2	1.7	1.5	1.4	1.3	1.3	1.2
Hairpin χ^2	1	1.37	1.54	1.64	1.70	1.74	1.77	1.79	1.80	1.81	1.82
	2	6.15	2.91	4.37	5.39	6.12	6.68	7.12	7.47	7.76	8.00
	3	22.93	9.12	3.69	5.98	7.41	8.42	9.18	9.76	10.23	10.60
	4	30.71	24.64	11.99	3.47	6.42	8.00	9.01	9.73	10.26	10.67

Table S3. Results of fitting our measurements of the unwinding rate in the hairpin and occluded-strand assays to the theoretical active model of helicase unwinding (Eqs. 8 and 9). We fit u/r as a function of force to U with different values of n and N, and fix $a = 0.05$ as was done in prior work (21). The parameter $0 < a < 1$ must be small in order for the helicase not to be significantly slowed by the repulsive potential (19, 20), and other small values $a \leq 0.2$ do not appreciably alter these fit results. Shown here are the best fit values of the "active" interaction energy U/k_BT and corresponding values of the minimized reduced χ^2. Good fits are shaded (arbitrary χ^2 cutoff), and best fits are darkly shaded. For hairpin unwinding, the best fit (see main text Fig. 3*A*) corresponds to $n = 1$ bp and $N = 1$ bp, with $U/k_BT = 0.5 \pm 0.1$. For the occluded-strand assay, the best fit (see main text Fig. 3*B*) corresponds to $n = 1$ bp and $N = 2$ bp, with $U/k_BT = 1.6 \pm 0.1$. These best fits are not highly dependent on N ($N > 10$ for $n = 1$ also provide good fits in both assays). Also, the data are reasonably well fit by an active model with step size $n = 2$ bp and larger U in both assays.

Supporting References

1. Lionnet, T., M. M. Spiering, S. J. Benkovic, D. Bensimon, and V. Croquette. 2007. Real-time observation of bacteriophage T4 gp41 helicase reveals an unwinding mechanism. *Proc. Natl. Acad. Sci. USA.* 104:19790-19795.
2. Bujalowski, W., and M. J. Jezewska. 1995. Interactions of *Escherichia coli* primary replicative helicase DnaB protein with single-stranded DNA. The nucleic acid does not wrap around the protein hexamer. *Biochemistry.* 34:8513-8519.
3. Smith, S. B., L. Finzi, and C. Bustamante. 1992. Direct mechanical measurements of the elasticity of single DNA molecules by using magnetic beads. *Science.* 258:1122-1126.
4. Saleh, O. A., D. B. McIntosh, P. Pincus, and N. Ribeck. 2009. Nonlinear low-force elasticity of single-stranded DNA molecules. *Phys. Rev. Lett.* 102:068301.
5. McIntosh, D. B., N. Ribeck, and O. A. Saleh. 2009. Detailed scaling analysis of low-force polyelectrolyte elasticity. *Phys. Rev. E.* 80:041803.
6. Berg-Sorensen, K., and H. Flyvbjerg. 2004. Power spectrum analysis for optical tweezers. *Rev. Sci. Instrum.* 75:594-612.
7. Bustamante, C., J. F. Marko, E. D. Siggia, and S. Smith. 1994. Entropic elasticity of lambda phage DNA. *Science.* 265:1599-1600.
8. Odijk, T. 1995. Stiff chains and filaments under tension. *Macromolecules.* 28:7016-7018.
9. Wang, M. D., H. Yin, R. Landick, J. Gelles, and S. M. Block. 1997. Stretching DNA with optical tweezers. *Biophys. J.* 72:1335-1346.
10. Baumann, C. G., S. B. Smith, V. A. Bloomfield, and C. Bustamante. 1997. Ionic effects on the elasticity of single DNA molecules. *Proc. Natl. Acad. Sci. USA.* 94:6185-6190.
11. Williams, M. C., J. R. Wenner, I. Rouzina, and V. A. Bloomfield. 2001. Entropy and heat capacity of DNA melting from temperature dependence of single molecule stretching. *Biophys. J.* 80:1932-1939.

12. Smith, S. B., Y. J. Cui, and C. Bustamante. 1996. Overstretching B-DNA: The elastic response of individual double-stranded and single-stranded DNA molecules. *Science.* 271:795-799.
13. Dessinges, M. N., B. Maier, Y. Zhang, M. Peliti, D. Bensimon, and V. Croquette. 2002. Stretching single stranded DNA, a model polyelectrolyte. *Phys. Rev. Lett.* 89:248102.
14. Tanner, N. A., S. M. Hamdan, S. Jergic, P. M. Schaeffer, N. E. Dixon, and A. M. van Oijen. 2008. Single-molecule studies of fork dynamics in *Escherichia coli* DNA replication. *Nat. Struct. Mol. Biol.* 15:170-176.
15. Galletto, R., M. J. Jezewska, and W. Bujalowski. 2004. Unzipping mechanism of the double-stranded DNA unwinding by a hexameric helicase: Quantitative analysis of the rate of the dsDNA unwinding, processivity and kinetic step-size of the *Escherichia coli* DnaB helicase using rapid quench-flow method. *J. Mol. Biol.* 343:83-99.
16. Higuchi, K., T. Katayama, S. Iwai, M. Hidaka, T. Horiuchi, and H. Maki. 2003. Fate of DNA replication fork encountering a single DNA lesion during oriC plasmid DNA replication in vitro. *Genes to Cells.* 8:437-449.
17. McInerney, P., and M. O'Donnell. 2004. Functional uncoupling of twin polymerases - Mechanism of polymerase dissociation from a lagging-strand block. *J. Biol. Chem.* 279:21543-21551.
18. Pages, V., and R. P. Fuchs. 2003. Uncoupling of leading- and lagging-strand DNA replication during lesion bypass in vivo. *Science.* 300:1300-1303.
19. Betterton, M. D., and F. Julicher. 2003. A motor that makes its own track: Helicase unwinding of DNA. *Phys. Rev. Lett.* 91:258103.
20. Betterton, M. D., and F. Julicher. 2005. Opening of nucleic-acid double strands by helicases: Active versus passive opening. *Phys. Rev. E.* 71:011904.
21. Johnson, D. S., L. Bai, B. Y. Smith, S. S. Patel, and M. D. Wang. 2007. Single-molecule studies reveal dynamics of DNA unwinding by the ring-shaped T7 helicase. *Cell.* 129:1299-1309.